

Large and dynamical tuning of a chalcogenide Fabry-Perot cavity mode by temperature modulation

Mecit Yaman,¹ H. Esat Kondakci,^{1,2} and Mehmet Bayindir^{1,2*}

¹UNAM-Institute of Materials Science and Nanotechnology,

²Department of Physics, Bilkent University, 06800 Ankara, Turkey

*bayindir@nano.org.tr

<http://bg.bilkent.edu.tr>

Abstract: Te-enriched chalcogenide glass Ge₁₅As₂₅Se₁₅Te₄₅ (GAST) is synthesized, thermo-optically characterized and used to fabricate a one dimensional photonic crystal cavity mode that is dynamically and reversibly tuned by temperature modulation. The optical cavity mode is designed using GAST and As₂S₃ glasses after fully determining their temperature dependence of the complex refractive indices in the visible and near infrared spectrum using spectroscopic ellipsometry. By making use of the very large thermo-optic coefficient ($dn/dT = 4 \times 10^{-4}/^{\circ}\text{C}$) of GAST glass at 1.2 μm , the cavity mode of the multilayer was tuned reversibly more than 16 nm, which is, to the best of our knowledge, an order of magnitude larger for this kind of cavity modulation. Wide and dynamical spectral tuning of low bandgap chalcogenide glasses via temperature modulation can be utilized in photonic crystal based integrated optics, quantum dot resonance matching, solid state and gas laser components, and infrared photonic crystal fibers.

© 2010 Optical Society of America

OCIS codes: (230.5298) Photonic crystals; (230.5750) Resonators; (160.6840) Thermo-optical materials.

References and links

1. J. D. Joannopoulos, S. G. Johnson, J. N. Winn, and R. D. Meade, P. R. Villeneuve, S. Fan, and J. D. Joannopoulos, *Photonic Crystals: Molding the Flow of Light*, Second ed. (Princeton: Princeton University Press, 2008).
2. S. Noda, A. Chutinan, and M. Imada, "Trapping and emission of photons by a single defect in a photonic bandgap structure," *Nature* **407**, 608–610 (2000).
3. M. Bayindir, A. F. Abouraddy, O. Shapira, J. Viens, D. Saygin-Hinczewski, F. Sorien, J. Arnold, J. D. Joannopoulos, and Y. Fink, "Kilometer-long ordered nanophotonic devices by preform-to-fiber fabrication," *IEEE J. Sel. Top. Quantum Electron.* **12**, 1202–1213 (2006).
4. A. F. Abouraddy, M. Bayindir, G. Benoit, S. D. Hart, K. Kuriki, N. Orf, O. Shapira, F. Sorin, B. Temelkuran, and Y. Fink, "Towards multimaterial multifunctional fibres that see, hear, sense and communicate," *Nature Mat.* **6**, 336–347 (2007).
5. A. Salimnia, T. Galstian, A. Villeneuve, K. Le Foulgoc, and K. Richardson, "Temperature dependence of Bragg reflectors in chalcogenide As₂S₃ glass slab waveguides," *J. Opt. Soc. Am. B* **17**, 1343–1348 (2000).
6. H. M. H. Chong, R. M. De La Rue, "Tuning of photonic crystal waveguide microcavity by thermo-optic effect," *IEEE Photon. Technol. Lett.* **16**, 1528–1530 (2004).
7. S. Song, S. S. Howard, Z. Liu, A. O. Dirisu, C. F. Gmachl, and C. B. Arnold, "Mode tuning of quantum cascade lasers through optical processing of chalcogenide glass claddings," *Appl. Phys. Lett.* **89**, 041115 (2006).
8. M. W. Lee, C. Grillet, C. L. C. Smith, D. J. Moss, B. J. Eggleton, D. Freeman, B. Luther-Davies, S. Madden, A. Rode, Y. Ruan, and Y. Lee, "Photosensitive post tuning of chalcogenide photonic crystal waveguides," *Opt. Express* **15**, 1277–1285 (2007).

9. A. Faraon, D. Englund, D. Bulla, B. Luther-Davies, B. J. Eggleton, N. Stoltz, P. Petroff, and J. Vuckovic, "Local tuning of photonic crystal cavities using chalcogenide glasses," *Appl. Phys. Lett.* **92**, 043123 (2008).
10. G. Benoit, K. Kuriki, J. F. Viens, J. D. Joannopoulos, and Y. Fink, "Dynamic all-optical tuning of transverse resonant cavity modes in photonic bandgap fibers," *Opt. Lett.* **30**, 1620–1622 (2005).
11. A. Faraon, J. Vuckovic, "Local temperature control of photonic crystal devices via micron-scale electrical heaters," *Appl. Phys. Lett.* **95**, 043102 (2009).
12. C. Grillet, C. Monat, C. L. Smith, M. W. Lee, S. Tomljenovic-Hanic, C. Karnutsch, and B. J. Eggleton, "Reconfigurable photonic crystal circuits," *Laser Photon. Rev.*, 1–13 (2009).
13. T. Asona, W. Kunishi, M. Nakamura, B.S. Song, and S. Noda, "Dynamical wavelength tuning of channel-drop device in two dimensional photonic crystal slab," *Electron. Lett.* **41**, 1–2 (2005).
14. I. Marki, M. Salt, H. P. Herzig, R. Stanley, L. El Melhaoui, P. Lyan, and J. M. Fedeli, "Optically tunable micro-cavity in a planar photonic crystal silicon waveguide buried in oxide," *Opt. Lett.* **31**, 513–515 (2006).
15. J. S. Sanghera and I. D. Aggarwal, "Active and passive chalcogenide glass optical fibers for IR applications: A review," *J. Non-Cryst. Solids* **257**, 6–16 (1999).
16. A. Zakery and S. R. Elliott, "Optical properties and applications of chalcogenide glasses: A review," *J. Non-Cryst. Solids* **330**, 1–12 (2003).
17. H. E. Kondakci, M. Yaman, O. Koylu, A. Dana, and M. Bayindir, "All-chalcogenide glass omnidirectional photonic band gap variable infrared filters," *Appl. Phys. Lett.* **94**, 11110 (2009).
18. G. Pfeiffer, M. A. Paesler, and S. C. Agarwal, "Reversible photodarkening of amorphous arsenic chalcogens," *J. Non-Cryst. Solids* **130**, 111–143 (1991).
19. K. Suzuki, Y. Hamachi, and T. Baba, "Fabrication and characterization of chalcogenide glass photonic crystal waveguides," *Opt. Express* **17**, 22393–22400 (2009).
20. D. Freeman, C. Grillet, M. W. Lee, C. L. C. Smith, Y. Ruan, A. Rode, M. Krolikowska, S. Tomljenovic-Hanic, C. M. De Sterke, M. J. Steel, B. Luther-Davies, S. Madden, D. J. Moss, Y. H. Lee, and B. J. Eggleton, "Chalcogenide glass photonic crystals," *Photon. Nanostructures* **6**, 3–11 (2008).
21. M. Asobe, T. Kanamori, and K. Kubodera, "Applications of highly nonlinear chalcogenide glass fibers in ultrafast all-optical switches," *IEEE J. Quantum Electron.* **29**, 2325–2333 (1993).
22. V. G. Taeed, L. Fu, M. Pelusi, M. Rochette, I. C. Littler, D. J. Moss, and B. J. Eggleton, "Error free all optical wavelength conversion in highly nonlinear As-Se chalcogenide glass fiber," *Opt. Express* **14**, 10371–10376 (2006).
23. M. Pelusi, F. Luan, T. D. Vo, M. R. E. Lamont, S. J. Madden, D. A. Bulla, D.-Y. Choi, B. Luther-Davies, and B. J. Eggleton, "Photonic-chip-based radio-frequency spectrum analyser with terahertz bandwidth," *Nat. Photonics* **3**, 139–143 (2009).
24. J. Hu, V. Tarasov, A. Agarwal, L. Kimerling, N. Carlie, L. Petit, and K. Richardson, "Fabrication and testing of planar chalcogenide waveguide integrated microfluidic sensor," *Opt. Express* **15**, 2307–2314 (2007).
25. G. Benoit, S. D. Hart, B. Temelkuran, J. D. Joannopoulos, and Y. Fink, "Static and dynamic properties of optical microcavities in photonic bandgap yarns," *Adv. Mat.* **15**, 2053–2056 (2003).
26. M. W. Lee, C. Grillet, S. Tomljenovic-Hanic, E. C. Magi, D. J. Moss, B. J. Eggleton, X. Gai, S. Madden, D.-Y. Choi, D. A. P. Bulla, and B. Luther-Davies, "Photowritten high-Q cavities in two-dimensional chalcogenide glass photonic crystals," *Opt. Lett.* **34**, 3671–3673 (2009).
27. A. R. Farouhi and I. Bloomer, "Optical dispersion relation for amorphous semiconductors and amorphous dielectrics," *Phys. Rev. B* **34**, 7018–7026 (1986).
28. S. Kugler, J. Hegedus, and K. Kohary, "Modelling of photoinduced changes in chalcogenide glasses: a-Se and a-As₂Se₃," *J. Mater. Sci.: Mater. Electron.* **18**, 163–167 (2007).

1. Introduction

Optical cavity modes, photonic bandgap structures with intentionally incorporated defects that break the periodicity to localize electromagnetic energy modes [1], provide basis for a large number of interesting passive and active devices both on chip [2] and in fiber [3,4]. A practical method is required for tuning optical cavities to make their spectra match well-defined resonances or to compensate fabrication imperfections [5–8], and also for fast and/or dynamical tuning to make active photonic components [10–14]. Optical cavities fabricated with amorphous chalcogenides are particularly of interest due to these glasses' optical, mechanical and thermal properties [15, 16]: chalcogenides make stable glasses that are infrared transmitting with a large transparency window (1–20 μm) and can be deposited using thermal evaporation [17]; they have relatively low glass transition temperatures (190–210°C); these glasses also exhibit low phonon energy and bandgap, high non-linearity, and high photo-sensitivity when illuminated by near bandgap light [18]. As a result chalcogenide based devices and optical fibers

have already found diverse applications in planar photonic crystals [8, 19, 20], all optical processing [21–23], as gratings and direct laser written waveguides [5], sensing applications [24], optically and mechanically tunable fibers [10, 25], and infrared fibers [15].

Recently attention has focused on the photo-induced and thermo-optical index tuning and modulation of chalcogenide based devices, e.g. photosensitivity of As_2S_3 is used for mode tuning of quantum cascade lasers using above bandgap illumination [7], for local tuning of photonic crystal cavities by photo-darkening [9], for post tuning of 2D photonic crystals with He-Ne laser [8], for cavity tuning of hollow core photonic crystal fibers by photodarkening [4] and Ge-As-Se was used recently for post tuning of high-Q two dimensional photonic crystals [26]. However in these studies the dynamical range of cavity modulation is limited to about 1-2 nm except for [26] in which a blue-shift of more than 10 nm is achieved after a 20.5 min exposure to a He-Ne laser intensity of 30 W/cm^2 . In this paper, we report thermo-optical characterization of a Tellurium-enriched chalcogenide glass $\text{Ge}_{15}\text{As}_{25}\text{Se}_{15}\text{Te}_{45}$ (GAST) with a very high thermo-optic coefficient, and demonstrate dynamical tuning of a wide dynamic range (16 nm), quarter wave stack based optical cavity fabricated using GAST and As_2S_3 chalcogenide glasses.

2. Optical characterization

The amorphous semiconductor glasses are prepared from high purity Ge, As, Se, and Te elements using conventional sealed-ampoule melt-quenching techniques [3]. We carried out a detailed characterization of the complex refractive indices, $\tilde{n}(\lambda, T) = n + ik$, of As_2S_3 and GAST thin films as a function of wavelength (400-1700 nm) and temperature (25-125 °C) by spectroscopic ellipsometry (J. A. Woollam, V-VASE) as shown in Fig. 1. As_2S_3 and GAST glasses were thermally evaporated stoichiometrically on different glass substrates (final thickness 120 nm, vacuum 10^{-6} Torr, rate $\sim 1 \text{ nm/s}$, Vaksis) [17]. Ellipsometric measurements were done with 25 °C interval, while heating from 25 to 125 °C, and also while cooling from 125 to 25 °C. The measurement cycle was repeated few times to observe any hysteresis.

The ellipsometric data were fit to a generalized oscillator model to obtain extinction coefficient, k and energy bandgap, E_g , at each wavelength using Tauc-Lorentz type optical absorption used for amorphous semiconductors $k(E) = A(E - E_g)^2 / (E^2 - BE + C)$, where A , B and C are non-zero constants characterizing the medium [27]. Real part of the index of refraction is then determined using Kramers-Kronig integrals to be $n(E) = n(\infty) + B_0E + C_0 / (E^2 - BE + C)$, where B_0 and C_0 are constants that depend on A , B , C and E_g . In addition to the complex refractive indices of the glasses, temperature dependence of the optical bandgap edge and film thicknesses were also obtained.

At room temperature As_2S_3 and GAST glasses have an optical absorption edge at 500 nm (2.48 eV) and 1204 nm (1.03 eV), respectively. A temperature change of 100 °C ($kT \approx 9 \text{ meV}$) results in a shift of both extinction coefficient profiles towards longer wavelengths. The optical absorption edge and bandgap energy E_g monotonically red-shifts for both glasses with increasing temperature. In terms of wavelengths the absorption edge of GAST shifts more (1204 to 1241) than As_2S_3 (500 to 502 nm). Extinction coefficient profile of As_2S_3 was found to be nearly constant in terms of wavelengths due the ultraviolet-visible absorption of the material [Fig. 1(a)].

After cooling, the absorption edge of GAST starts to increase again reaching 1176 nm (1.05 eV); corresponding to a 0.02 eV hysteresis after one heating and cooling cycle. The hysteresis in the bandgap and thickness suggest that structural changes took place due to cyclic heating (the thin films were not annealed after thermal deposition), as is well known for chalcogenide glasses [28]. Subsequent heating/cooling cycles did not result in a hysteresis of the E_g or extinction coefficient of the glasses. Shift in the extinction coefficient k manifests itself with a spec-

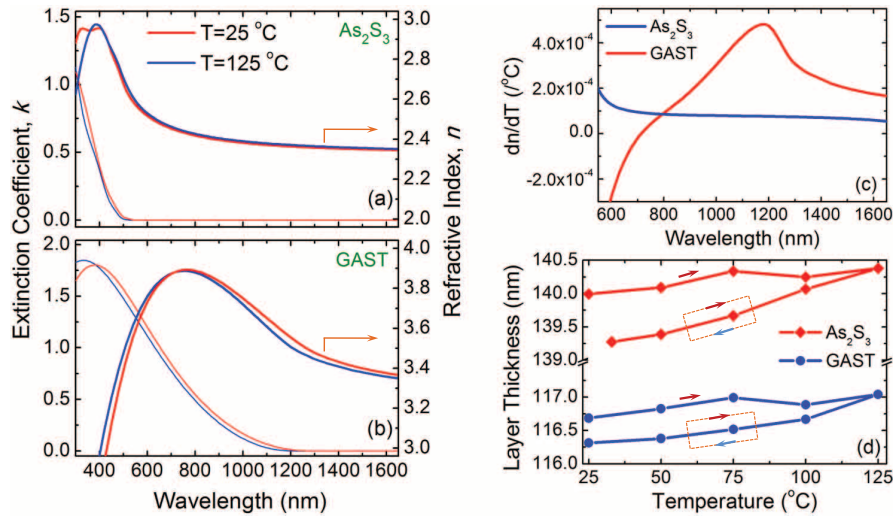


Fig. 1. The refractive index n , and extinction coefficient k , of (a) As_2S_3 and (b) GAST thin film chalcogenide glasses obtained by spectroscopic ellipsometry at 25 and 125°C. Both extinction coefficients shift to longer wavelengths with increasing temperature. The thermo-optic coefficient is higher for the GAST glass due to low bandgap energy, which also changes sign and becomes positive after 745 nm. (c) Spectroscopic thermo-optic coefficients of As_2S_3 and GAST glasses. (d) Measured thin film thicknesses as a function of temperature.

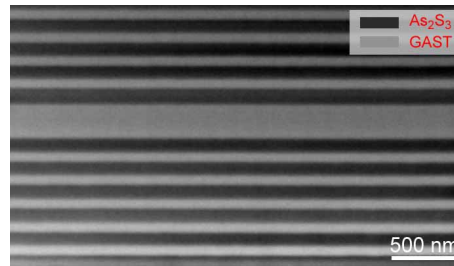


Fig. 2. The SEM picture of a one dimensional photonic crystal based optical cavity fabricated with high index contrast $\text{Ge}_{15}\text{As}_{25}\text{Se}_{15}\text{Te}_{45}$ and As_2S_3 chalcogenide glasses.

tral shift of the refractive index as well, thus resulting in negative thermo-optic coefficients ($\Delta n/\Delta T$) in the smaller wavelengths and positive for longer wavelengths. Accordingly, GAST glass is observed to have a negative thermo-optic coefficient for wavelengths smaller than 745 nm and positive thereafter. The refractive index change with temperature was extraordinarily high; for example, thermo-optic coefficient is $-3 \times 10^{-4}/^\circ\text{C}$ at $0.6 \mu\text{m}$ and $+4 \times 10^{-4}/^\circ\text{C}$ at $1.2 \mu\text{m}$ wavelengths [Fig. 1(a)–1(b)]. On the other hand, As_2S_3 has a thermo-optic coefficient of $+5 \times 10^{-5}/^\circ\text{C}$ at 0.7 and $1.2 \mu\text{m}$ wavelengths [Fig. 1(c)]. The film thickness, measured by the ellipsometer, is observed to increase with increasing temperature and decrease with cooling with a hysteresis of $0.4 \text{ nm} \pm 0.1 \text{ nm}$, corresponding to a thermal expansion coefficient two orders of magnitude high for the thin film chalcogenides compared to bulk counterparts $2 \times 10^{-3}/^\circ\text{C}$ versus $\sim 10^{-5}/^\circ\text{C}$, respectively [Fig. 1(d)].

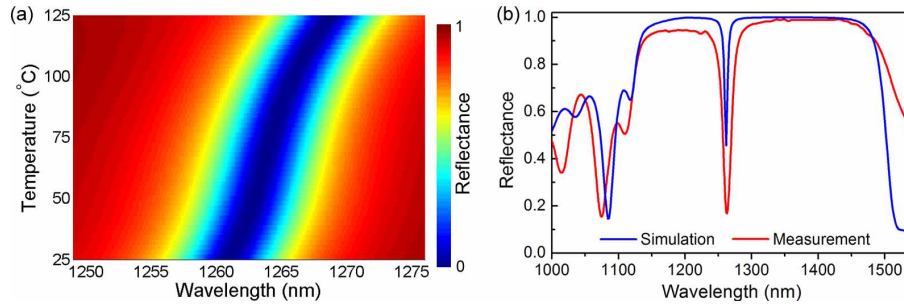


Fig. 3. (a) Simulation of the temperature dependence of the cavity mode between 25-125 °C in the cavity region. The cavity shifts towards larger wavelengths with increasing temperature. (b) Simulation and experimental results of the photonic band structure based on GAST and As₂S₃ glasses.

3. Device fabrication

Using the high temperature-dependence of the refractive index of GAST chalcogenide glass, a one dimensional photonic crystal based optical cavity is designed. The optical cavity is composed of 7+7 bilayers of As₂S₃ and GAST layers, 136 nm and 93 nm thickness respectively, with a 137 nm GAST defect layer (Fig. 2). The cavity layer thickness is selected to achieve maximum cavity shift when exposed to temperature rise, using a modified Transfer Matrix Method (TMM) which includes temperature dependence of the refractive indices. According to the simulations, 0.4 μm wide stop band with a cavity layer at 1260 nm shifts 16 nm towards higher wavelengths [Fig. 3(a)]. Next, the optical cavity is fabricated according to simulation results. The multilayer structure is deposited layer by layer on a standard microscope slide. The reflectance spectrum of the multilayer structure was obtained using a spectroscopic ellipsometer in reflection mode. The measured band and cavity agree well with simulation results [Fig. 3(b)]. Slight deviations might be due to small thickness fluctuations while fabricating the multilayer structure.

4. Results and discussion

Dynamical behavior of the cavity mode is investigated using spectroscopic ellipsometry with a heating stage, in reflection mode, 25° incidence angle. The oblique incidence angle slightly shifts the cavity mode to be 1254 nm which was required for mounting the heating stage on the ellipsometer. Temperature of the multilayer structure was taken up to 125°C by 25°C temperature steps during which temperature measurements were taken after the controller temperature was stabilized. The corresponding thermal expansion was measured to be well below 0.01% for all layers. The cavity mode, which is at 1254 nm at room temperature, is observed to shift monotonically towards higher wavelengths with increasing temperature and, conversely towards shorter wavelengths with decreasing temperature as shown in Fig. 4(a). The cavity shift rate was 0.1 nm/°C with a total shift of 16 nm around 1254 nm, corresponding to a maximum change in reflectivity of 70% at 1254 nm. The experimental results of the cavity mode shift with dynamical thermal tuning agree well with our temperature and extinction coefficient included TMM simulations indicating the effect of the thermo-optic coefficient. However the linewidth of the cavity mode appears to be slightly widening which is not apparent from our simulations due to the cavity mode quality factor. The slight widening could be due to the red-shift of the extinction coefficient which must be further explored. The dynamical tuning effect was observed to be repeatable after many heating and cooling cycles. Also, after the first full

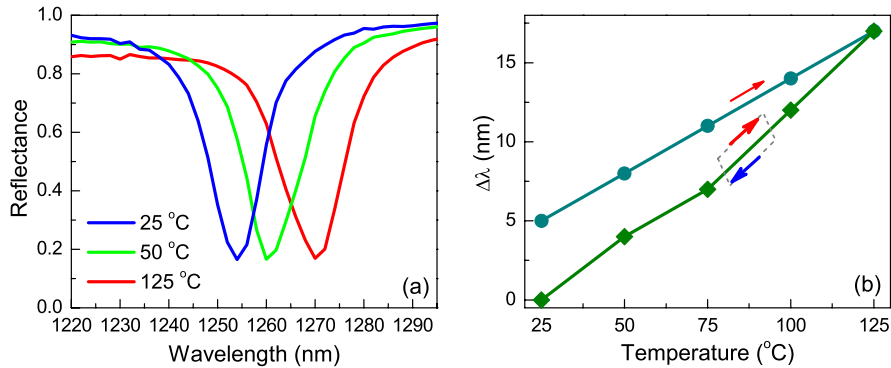


Fig. 4. (a) Reversible tuning of photonic band gap cavity mode by temperature modulation with a dynamical range of 16 nm. (b) The cavity mode shifts to longer (shorter) wavelengths by increasing (decreasing) temperature. The hysteresis is removed with the first heating/cooling cycle after which the cavity follows the lower path.

heating/cooling cycle a 5 nm hysteresis is observed, resulting in an increase in the dynamic range of the tuning, which stayed constant for the subsequent heating cycles [Fig. 4(b)]. As discussed before, the hysteresis can be avoided by first annealing the sample before dynamical tuning.

5. Conclusion

We presented to the best of our knowledge the first ellipsometric determination of the complex refractive index of $\text{Ge}_{15}\text{As}_{25}\text{Se}_{15}\text{Te}_{45}$ (GAST) and As_2S_3 chalcogenide glasses and largest dynamical range thermal modulation of an optical cavity fabricated with these glasses. It was demonstrated that upon temperature change the refractive indices of amorphous semiconductors change according to the extinction coefficient shift which depends on the electronic bandgap of the material; lower the electronic bandgap, higher the refractive index change around the absorption edge. It was found that for these materials dn/dT coefficients are negative for shorter wavelengths and positive for longer wavelengths. Using high thermo-optic coefficient GAST glass, reversible tuning of an optical cavity with a large dynamic range of 16 nm at near infrared wavelengths was demonstrated on chip, which is an order of magnitude larger compared to previously achieved cavity shifts with non-Telluride chalcogenides [9, 10]. Same high thermo-optic coefficient Telluride chalcogenide glass can also be used in other active devices both on chip and in fiber.

Acknowledgements

The authors thank M. Vural for helpful conversations, B. Kaplan for the introduction of the generalized oscillator model analysis with ellipsometer, M. H. Dolas for his help with the multi-layer fabrication and K. Mizrak for the SEM micrographs. This work is supported by TUBITAK under the Project No. 106G090. MB acknowledges support from the Turkish Academy of Sciences Distinguished Young Scientist Award (TUBA GEBIP). This work was performed at UNAM-Institute of Materials Science and Nanotechnology supported by the State Planning Organization of Turkey through the National Nanotechnology Research Center Project.